Genome Sequence Archive in BIG Data Center, Beijing Institute of Genomics, Chinese Academy of Sciences, under project PRJCA002557. The accession number is HRA000145. Further information about sequencing data can be found at https://bigd.big.ac.cn/gsa-human/browse/HRA000145.

[1]Shandong Provincial Hospital for Skin Diseases and Shandong Provincial Institute of Dermatology and Venereology, Shandong First Medical University & Shandong Academy of Medical Sciences, Jinan, Shandong, China
*Corresponding author e-mail: hongyue2519@hotmail.com

ORCIDs

Xiaotong Xue: http://orcid.org/0000-0002-2990-0745
Zihao Mi: http://orcid.org/0000-0002-2912-6374
Zhenzhen Wang: https://orcid.org/0000-0001-5927-2471
Zheng Pang: https://orcid.org/0000-0001-7800-1124
Hong Liu: https://orcid.org/0000-0003-4488-0372
Furen Zhang: https://orcid.org/0000-0002-3383-1973

CONFLICT OF INTEREST

The authors state no conflict of interest.

ACKNOWLEDGMENTS

AUTHOR CONTRIBUTIONS

Conceptualization: FZ, HL; Formal Analysis: ZW; Funding Acquisition: FZ; Methodology: HL, XX, ZM; Writing - Original Draft: XX; Writing - Review and Editing: FZ, HL, ZP

Xiaotong Xue[1], Zihao Mi[1], Zhenzhen Wang[1], Zheng Pang[1], Hong Liu[1,] and Furen Zhang[1]*

SUPPLEMENTARY MATERIAL

Supplementary material is linked to the online version of the paper at www.jidonline.org, and at https://doi.org/10.1016/j.jid.2020.05.087.

REFERENCES

Boguniewicz M, Leung DY. Atopic dermatitis: a disease of altered skin barrier and immune dysregulation. Immunol Rev 2011;242:233–46.

Hamming I, Timens W, Bulthuis ML, Lely AT, Navis G, van Goor H. Tissue distribution of ACE2 protein, the functional receptor for SARS coronavirus. A first step in understanding SARS pathogenesis. J Pathol 2004;203:631–7.

Haque A, Engel J, Teichmann SA, Lönnberg T. A practical guide to single-cell RNA-sequencing for biomedical research and clinical applications. Genome Med 2017;9:75.

Hoffmann M, Kleine-Weber H, Schroeder S, Krüger N, Herrler T, Erichsen S, et al. SARS-CoV-2 cell entry depends on ACE2 and TMPRSS2 and is blocked by a clinically proven protease inhibitor. Cell 2020;181:271–80.e8.

Huang C, Wang Y, Li X, Ren L, Zhao J, Hu Y, et al. Clinical features of patients infected with 2019 novel coronavirus in Wuhan, China. Lancet 2020;395:497–506.

Liang W, Feng Z, Rao S, Xiao C, Xue X, Lin Z, et al. Diarrhoea may be underestimated: a missing link in 2019 novel coronavirus. Gut 2020;69:1141–3.

Lukassen S, Chua RL, Trefzer T, Kahn NC, Schneider MA, Muley T, et al. SARS-CoV-2 receptor ACE2 and TMPRSS2 are primarily expressed in bronchial transient secretory cells. EMBO J 2020;39:e105114.

Park SE. Epidemiology, virology, and clinical features of severe acute respiratory syndrome-coronavirus-2 (SARS-CoV-2; coronavirus disease-19). Clin Exp Pediatr 2020;63:119–24.

Recalcati S. Cutaneous manifestations in COVID-19: a first perspective. J Eur Acad Dermatol Venereol 2020;34:e212–3.

To KK, Tsang OT, Leung WS, Tam AR, Wu TC, Lung DC, et al. Temporal profiles of viral load in posterior oropharyngeal saliva samples and serum antibody responses during infection by SARS-CoV-2: an observational cohort study. Lancet Infect Dis 2020;20:565–74.

Wang Q, Zhang Y, Wu L, Niu S, Song C, Zhang Z, et al. Structural and functional basis of SARS-CoV-2 entry by using human ACE2. Cell 2020;181:894–904.e9.

Wrapp D, Wang N, Corbett KS, Goldsmith JA, Hsieh CL, Abiona O, et al. Cryo-EM structure of the 2019-nCoV spike in the prefusion conformation. Science 2020;367:1260–3.

Xu H, Zhong L, Deng J, Peng J, Dan H, Zeng X, et al. High expression of ACE2 receptor of 2019-nCoV on the epithelial cells of oral mucosa. Int J Oral Sci 2020a;12:8.

Xu X, Chen P, Wang J, Feng J, Zhou H, Li X, et al. Evolution of the novel coronavirus from the ongoing Wuhan outbreak and modeling of its spike protein for risk of human transmission. Sci China Life Sci 2020b;63:457–60.

Yan Y, Chen H, Chen L, Cheng B, Diao P, Dong L, et al. Consensus of Chinese experts on protection of skin and mucous membrane barrier for health-care workers fighting against coronavirus disease 2019 [e-pub ahead of print]. Dermatol Ther 2020. https://doi.org/10.1111/dth.13310 (accessed 13 Mar 2020).

Inflammasome Activation by CD8+ T Cells from Patients with Cutaneous Leishmaniasis Caused by *Leishmania braziliensis* in the Immunopathogenesis of the Disease

TO THE EDITOR

Cutaneous leishmaniasis (CL) is characterized by an inflammatory response mainly mediated by CD4+ T cells producing IFN-γ, which are responsible for macrophage activation and intracellular Leishmania *braziliensis* parasite killing. We recently showed the importance of CD8+ T cells in the pathogenesis of human CL as skin lesions from patients with CL present higher frequencies of CD8+ T cells, contributing to the inflammatory response (Cardoso et al., 2015; Santos et al., 2013). Moreover, lesion size was found to positively correlate with the frequency of CD8+ T cells–expressing granzyme B. The cytotoxic response mediated by CD8+ T cells was not found to be linked to decreased parasite load in human macrophages infected in vitro (Cardoso et al., 2015; Santos et al., 2013).
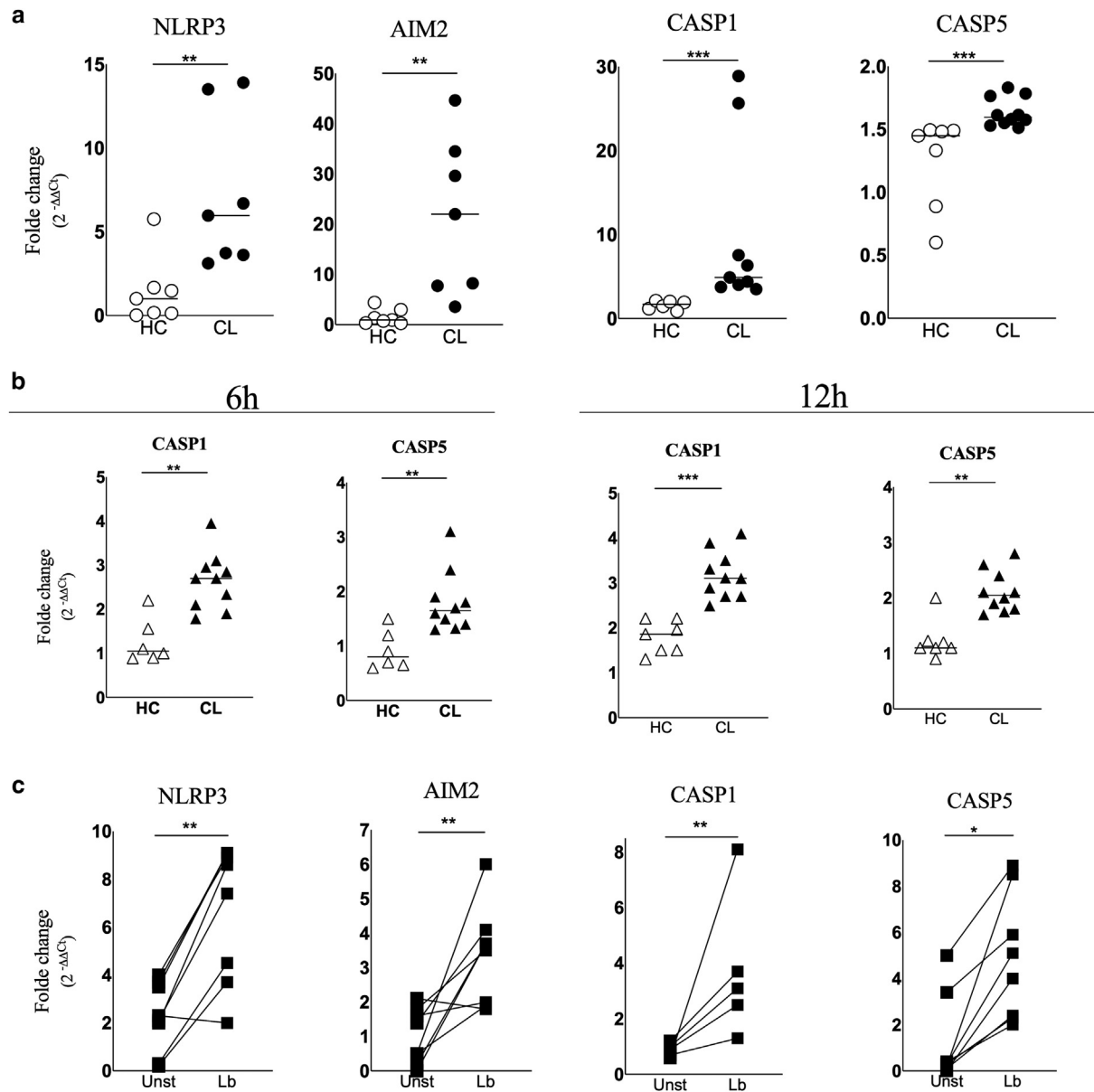
Figure 1. Elevated expression of inflammasome platform in CL skin lesions, PBMC, and macrophages and/or CD8 Cocultures. Relative expression of caspases in skin samples, PBMCs, and macrophages and/or CD8^{+} cocultures from patients with CL detected by RT-qPCR. Relative gene expression of *NLRP3*, *AIM2*, *CASP*-1, and *CASP*-5 in cutaneous lesions from patients with CL. (**a**) Relative gene expression of *CASP*-1 and *CASP*-5 in PBMCs from patients with CL (**b**) 6 h and (**b**) 12 h after stimulation with promastigotes of *Leishmania (Viannia) braziliensis*. (**c**) Relative gene expression of *NLRP3*, *AIM2*, *CASP*-1, and *CASP*-5 in macrophages and/or CD8^{+} cocultures from patients with CL 12 h after stimulation with promastigotes of *L.(V.) braziliensis*. Relative expression assessed by [ΔΔ]CT using skin samples from HCs. [ΔΔ]CT, comparative CT method; CL, cutaneous leishmaniasis; CT, computed tomography; h, hour; HC, healthy control; Lb, *Leishmania braziliensis*; Unst, unstimulated.

Recently, some authors have stated that CD8^{+} T cells mediate tissue damage through the activation of NLRP3, leading to IL-1β secretion in *L. braziliensis*–infected mouse models and cells obtained from human CL skin lesions (Novais et al., 2017). Here, we evaluated the ability of CD8^{+} T cells to induce inflammasome expression and activation in cells from patients with CL and establish correlations with healing time. This study was approved by the Ethics and Research Committee from the Federal University of Bahia, Brazil, and the National Commission of Ethics in Research (39324114.0.0000.5577). All individuals were volunteer adults and provided written informed consent. A detailed description of the methods is presented in the Supplementary Materials and Methods.
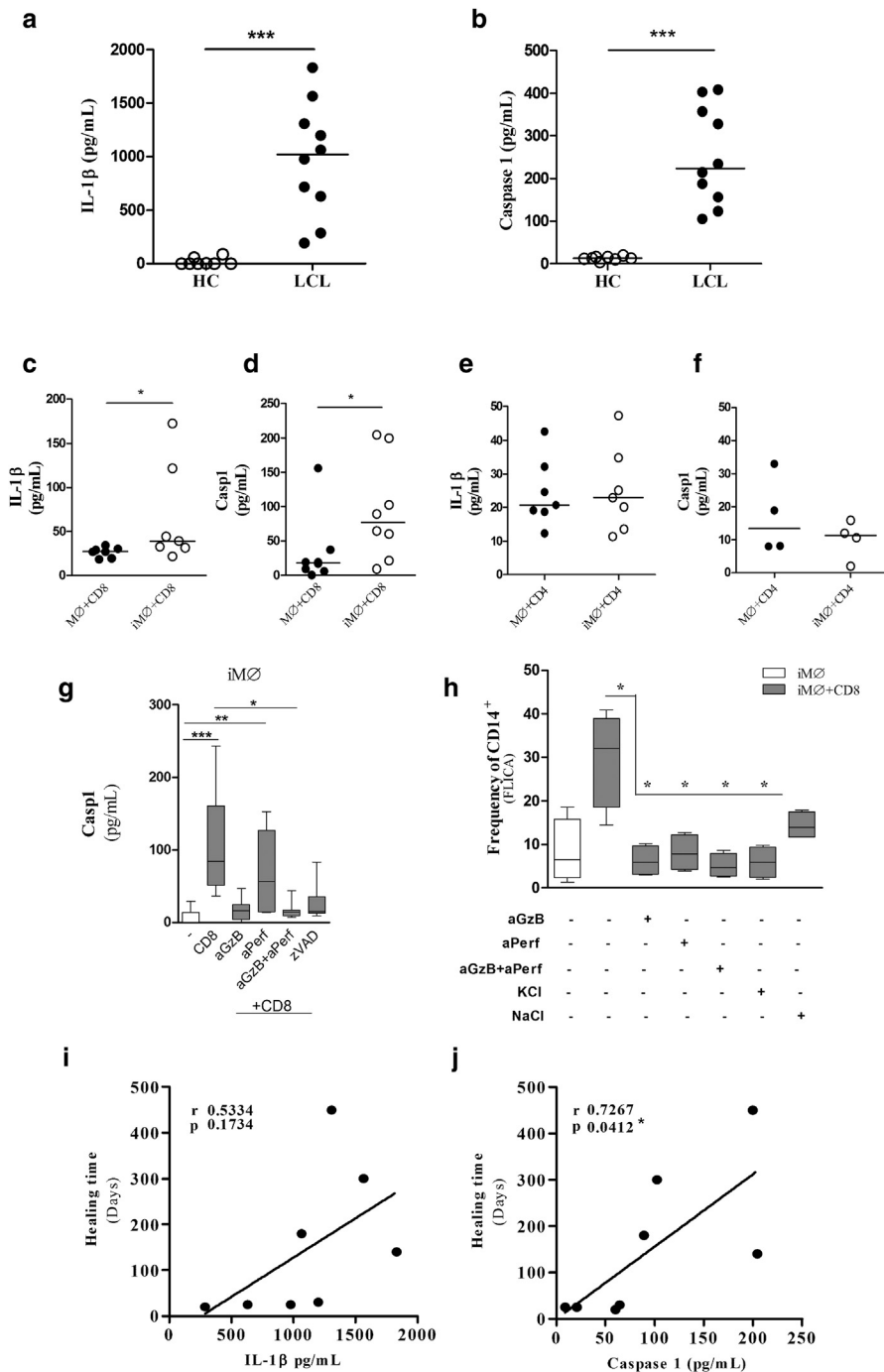
Increased expression of NLRP3, AIM2, and CASP-1/5 was observed by qPCR in CL skin lesions compared with healthy skin samples (Figure 1a). Increased CASP-1/5 expression was also observed in PBMCs obtained from patients with CL stimulated with *L. (Viannia) braziliensis* after 6 and 12 hours of culture (Figure 1b). To determine the role of CD8^{+} T cells in increased inflammasome expression, these cells were cocultured with *L. braziliensis*–infected macrophages. After 12 hours of coculture, increased expression of NLRP3, AIM2, and CASP-1/5 was observed compared with

Figure 2. IL-1β and CASP-1 produced in macrophage and/or CD8^{+} T coculture from patients correlates with healing time. (a) IL-1β and (b) CASP-1 were measured by ELISA after 72 h of biopsy cultures. (c, e) IL-1β and (d, f) CASP-1 from macrophage and/or CD8^{+} or CD4^{+} T-cell cocultures were measured by ELISA. CD8^{+} or CD4^{+} T cells were purified from PBMCs of patients with CL and cocultured with uninfected or infected macrophages for (c–f). 12 h. (g) Active CASP-1 secretion and (h) intracellular active CASP-1 (FLICA) measured in autologous cocultures from patients with CL for 12 h after *Leishmania (V.) braziliensis* stimulation in the presence of (g, h) granzyme B and/or perforin inhibitors and (h) KCl or NaCl hyperosmotic medium. Relationship between (i) IL-1β and healing time Pearson's $r = 0.5334$ as well as (j) CASP-1 and time healing Pearson's $r = 0.7267$. aGZB, anti-granzyme B; aPerf, anti-perforin; CL, cutaneous leishmaniasis; h, hour; HC, healthy control; KCl, potassium chloride; NaCl, sodium chloride; zVAD, carbobenzoxy-valyl-alanyl-aspartyl-[O-methyl]-fluoromethylketone.

2018). CASP-1 is responsible for converting proinflammatory cytokines, such as IL-1β and IL-18, into their mature and active form, thereby favoring cytokine release and inflammation (Howard et al., 1997; Place and Kanneganti, 2018). Our results showed elevated expression of inflammasome components NLRP3 and AIM2 in patients with CL skin lesions, which could explain the upregulation of inflammatory *CASP* genes observed herein. Concurrently, some reports have described NLR activation by different species of *Leishmania* in vitro and in vivo (Charmoy et al., 2016; Lima-Junior et al., 2013; Santos et al., 2018)

To validate our expression data, IL-1β and CASP-1 levels were measured in biopsied cell cultures for 12 hours. Increased production of IL-1β (Figure 2a) and CASP-1 (Figure 2b) was seen in the supernatant of CL biopsy cultures compared with that of healthy controls. To confirm our results regarding inflammasome activation by CD8^{+} T cells, *L. braziliensis*–infected macrophages were cocultured with CD8^{+} T cells from patients with CL for 12 hours, followed by the assessment of IL-1β and CASP-1 secretion. We found increased levels of IL-1β and CASP-1 in autologous cocultures (CD8^{+} T cells + macrophages from patients with CL) in contrast to cocultured uninfected macrophages (Figures 2c–d). In addition, *L. braziliensis*–infected macrophages alone (Figures 2g–h) or those cocultured with CD4^{+} T cells did not induce CASP-1 or IL-1β secretion compared with cocultured uninfected macrophages (Figures 2e–f).

It is well-known that during the cytolytic process, CD8^{+} T cells release perforin and granzyme-mediating apoptosis in target cells (Li et al., 2014). Accordingly, we hypothesized that perforin released by activated CD8^{+} T cells binds to the surface of target cells, triggering potassium ion imbalance, thereby leading to inflammasome activation. To test this, we inhibited granzyme B and perforin during the coculturing of *L. braziliensis*–infected macrophages and CD8^{+} T cells or added a hyperosmotic medium containing 50 μM potassium chloride or sodium chloride. The inhibition of granzyme B and perforin reduced active CASP-1 secretion

uninfected cell cultures (Figure 1c). The activation of these molecules contributes to the pathophysiology of several

diseases, including leishmaniasis (Ferraz et al., 2015; Hyman and Yuan, 2012; Novais et al., 2015; Santos et al.,

levels and YVAD-FLICA—positive cells during infected macrophages and CD8^{+} T-cell cocultures (Figures 2g—h). This reduction suggested that CD8^{+} T cells may induce potassium efflux and, consequently, inflammasome activation. In contrast, in cocultures of CD4^{+} T cells and infected macrophages, no significant differences were found in CASP-1 and IL-1β production.

In addition, increases in extracellular potassium ion by potassium chloride were shown to reduce the activation of CASP-1 in CD14^{+} cells (Figure 2h). These results indirectly suggest that the cytolytic process in the membranes of target cells caused by perforin do indeed induce a potassium ion efflux. Potassium efflux is a remarkable signal involved in the activation of the NLRP3 inflammasome and inflammatory caspases (Muñoz-Planillo et al., 2013).

Recent work described the value of inflammasome platforms in predicting treatment outcome in CL (Amorim et al., 2019). To investigate whether CASP-1 and IL-1β production could be related to poor disease prognosis, we correlated the production of these proteins in the supernatant of infected macrophage and CD8^{+} T-cell cocultures with the healing time of each patient. CASP-1 but not IL-1β production presented a positive correlation with healing time (Figures 2i and j). The fact that CASP-1 secretion is linked to healing time supports the role of CD8^{+}-dependent inflammasome activation in worsening CL outcomes. Indeed, recent work demonstrates that patients presenting the higher expression of genes associated with cytotoxic T cells presented a poorer response to treatment in the healing of CL lesions (Amorim et al., 2019).

This study investigated the role of CD8^{+} T cells obtained from patients with CL in the activation of the inflammasome pathway. The increased inflammasome component expression observed in patients with CL indicates that this process may be related to tissue damage (Santos et al., 2018). Recent reports have highlighted the modulation of inflammasome activation as a possible target for treating tissue injury in this disease (Carvalho et al., 2020). Further studies will be crucial in determining methods of modulating the

inflammasome to design therapeutic targets against CL.

Data availability statement

No datasets were generated or analyzed during this study.

ORCIDs

Thiago Marconi Cardoso: http://orcid.org/0000-0002-0074-9789

Jonilson B. Lima: http://orcid.org/0000-0002-1403-4768

Ícaro Bonyek-Silva: http://orcid.org/0000-0002-0346-9360

Sara Nunes: http://orcid.org/0000-0001-8546-7598

Daniel Feijó: http://orcid.org/0000-0002-3552-8847

Hugo Almeida: http://orcid.org/0000-0002-6584-228X

Juliana Silva: http://orcid.org/0000-0002-5546-932X

Aldina Barral: http://orcid.org/0000-0002-7177-464X

Viviane Boaventura: http://orcid.org/0000-0002-7241-6844

Valéria M. Borges: http://orcid.org/0000-0002-2775-5409

Dario S. Zamboni: http://orcid.org/0000-0002-7856-7512

Lucas Pedreira de Carvalho: http://orcid.org/0000-0001-5033-1666

Edgar M. Carvalho: http://orcid.org/0000-0002-2697-8002

Natalia M. Tavares: http://orcid.org/0000-0002-4026-679X

Cláudia Brodskyn: http://orcid.org/0000-0003-3367-5365

CONFLICT OF INTEREST

The authors state no conflict of interest.

AUTHOR CONTRIBUTIONS

Conceptualization: TMC, JBL CB; Data Curation: TMC, NMT, CB; Formal Analysis: TMC, NMT, CB; Funding Acquisition: DF, CB; Investigation: TMC, IBS, SN, DF, HA, JBL; Methodology: TMC, JBL, DF, HA, JS; Project Administration: CB; Resources: AB, VB, VMB, DSZ, LPC, EMC, CB; Supervision: CB; Validation: TMC, NMT, CB; Visualization: TMC, JBL, NMT, CB; Writing - Original Draft Preparation: JBL, CB; Writing - Review and Editing: JBL, NMT, CB

Thiago Marconi Cardoso[1,2,3], *Jonilson B. Lima*[4], *Ícaro Bonyek-Silva*[1,5], *Sara Nunes*[1,5], *Daniel Feijó*[1], *Hugo Almeida*[1], *Juliana Silva*[2], *Aldina Barral*[1,6], *Viviane Boaventura*[1,5], *Valéria M. Borges*[1], *Dario S. Zamboni*[7], *Lucas Pedreira de Carvalho*[1,2,3], *Edgar M. Carvalho*[1,2,3], *Natalia*

M. Tavares[1,5,6] *and Cláudia Brodskyn*[1,5,6,*]

[1]Fiocruz-BA, Instituto Gonçalo Moniz, Salvador, Bahia, Brazil; [2]Serviço de Imunologia, Hospital Universitário Prof Edgar Santos, Universidade Federal da Bahia, Salvador, Bahia, Brazil; [3]Instituto Nacional de Ciência e Tecnologia de Doenças Tropicais - Instituto Nacional de Ciência e Tecnologia em - Doenças Tropicais (Conselho Nacional de Pesquisa/Ministério da Ciência e Tecnologia), Salvador, Bahia, Brazil; [4]Centro de Ciências Biológicas e da Saúde, Universidade Federal do Oeste da Bahia (UFOB); [5]Faculdade de Medicina da Universidade Federal da Bahia, Salvador, Bahia, Brazil; [6]Instituto Nacional de Ciência e Tecnologia de Instituto de Investigação de Imunologia (Conselho Nacional de Pesquisa/Ministério da Ciência e Tecnologia), São Paulo, Brazil; and [7]Faculdade de Medicina de Ribeirão Preto, Universidade de São Paulo, São Paulo, Brazil
*Corresponding author e-mail: claudia.brodskyn@fiocruz.br

SUPPLEMENTARY MATERIAL

Supplementary material is linked to the online version of the paper at www.jidonline.org, and at https://doi.org/10.1016/j.jid.2020.05.106.

REFERENCES

Amorim CF, Novais FO, Nguyen BT, Misic AM, Carvalho LP, Carvalho EM, et al. Variable gene expression and parasite load predict treatment outcome in cutaneous leishmaniasis. Sci Transl Med 2019;11:eaax4204.

Cardoso TM, Machado Á, Costa DL, Carvalho LP, Queiroz A, Machado P, et al. Protective and pathological functions of CD8+ T cells in *Leishmania braziliensis* infection. Infect Immun 2015;83:898—906.

Carvalho AM, Novais FO, Paixão CS, De Oliveira CI, Machado PR, Scott P, et al. Glyburide, a NLRP3 inhibitor, decreases inflammatory response and is a candidate to reduce pathology in *Leishmania braziliensis* infection. J Infect Dis 2020;140:246—9.e2.

Charmoy M, Hurrell BP, Romano A, Lee SH, Ribeiro-Gomes F, Riteau N, et al. The Nlrp3 inflammasome, IL-1β, and neutrophil recruitment are required for susceptibility to a non-healing strain of Leishmania major in C57BL / 6 mice. Eur J Immunol 2016;46:897—911.

Ferraz R, Cunha CF, Gomes-Silva A, Schubach AO, Pimentel MIF, Lyra MR, et al. Apoptosis and frequency of total and effector CD8+ T lymphocytes from cutaneous leishmaniasis patients during antimonial therapy. BMC Infect Dis 2015;15:74.

Howard AD, Kostura MJ, Thornberry N, Ding GJ, Weidner J, Salley JP, et al. IL-1-converting enzyme requires aspartic acid residues for processing of the IL-1 beta precursor at two distinct sites and does not cleave 31- kDa IL-1 alpha. J Immunol 1997;147:2964—9.

Hyman BT, Yuan J. Apoptotic and non-apoptotic roles of caspases in neuronal physiology and pathophysiology. Nat Rev Neurosci 2012;13:395—406.

Li XY, Li Z, An GJ, Liu S, Lai YD. Co-expression of perforin and granzyme B genes induces apoptosis and inhibits the tumorigenicity of laryngeal cancer cell line Hep-2. Int J Clin Exp Pathol 2014;7: 978−86.

Lima-Junior DS, Costa DL, Carregaro V, Cunha LD, Silva ALN, Mineo TWP, et al. Inflammasome-derived IL-1β production induces nitric oxide-mediated resistance to Leishmania. Nat Med 2013;19:909−15.

Muñoz-Planillo R, Kuffa P, Martínez-Colón G, Smith BL, Rajendiran TM, Núñez G. K$^+$ efflux is the common trigger of NLRP3 inflammasome activation by bacterial toxins and particulate matter. Immunity 2013;38:1142−53.

Novais FO, Carvalho AM, Clark ML, Carvalho LP, Beiting DP, Brodsky IE, et al. CD8+T cell cytotoxicity mediates pathology in the skin by inflammasome activation and IL-1β production. PLoS Pathog 2017;13: e1006196.

Novais FO, Carvalho LP, Passos S, Roos DS, Carvalho EM, Scott P, et al. Genomic profiling of human *Leishmania braziliensis* lesions identifies transcriptional modules associated with cutaneous immunopathology. J Invest Dermatol 2015;135:94−101.

Place DE, Kanneganti TD. Recent advances in inflammasome biology. Curr Opin Immunol 2018;50:32−8.

Santos CDS, Boaventura V, Ribeiro Cardoso C, Lordelo MJ, Tavares N, Noronha A, et al. CD8(+) granzyme B(+) -mediated tissue injury vs. CD4(+)IFNγ(+)-mediated parasite killing in human cutaneous leishmaniasis. J Invest Dermatol 2013;133: 1533−40.

Santos D, Campos TM, Saldanha M, Oliveira SC, Nascimento M, Zamboni DS, et al. IL-1β production by intermediate monocytes is associated with immunopathology in cutaneous leishmaniasis [published correction appears in J Invest Dermatol 2014 Nov;134(11):2850]. J Invest Dermatol 2018;138:1107−15.

Diagnostic Two-Gene Classifier in Early-Stage Mycosis Fungoides: A Retrospective Multicenter Study

TO THE EDITOR

Although mycosis fungoides (MF) is the most common cutaneous T-cell lymphoma, it still poses a major diagnostic challenge because of clinical and histological similarities to benign inflammatory dermatosis (BID), resulting in prolonged diagnostic workup (Scarisbrick et al., 2019). Algorithms based on clinical, morphological, immunophenotypical, and molecular parameters have added to diagnostic accuracy in early-stage disease (Pimpinelli et al., 2005). In addition, TOX, PDCD1, CADM1, BLK, and genes related to the TNF signaling pathway have been reported as potential diagnostic markers (Krejsgaard et al., 2009; Litvinov et al., 2017; Tracey et al., 2003; Yuki et al., 2018; Zhang et al., 2012). Decades of research have provided considerable evidence on the interaction between malignant T cells and benign immune and stromal cells, inhibiting antitumor responses while promoting tumor cell growth through the inflammatory microenvironment produced by the neoplastic cells and thereby driving the stage-related inflammation characteristic of MF (Krejsgaard et al., 2017).

Only a few studies have investigated the role of the innate immune cells (Cioplea et al., 2019). To this end, we performed gene expression analysis with emphasis on the innate immune system on 43 initial diagnostic biopsies from 36 patients with early-MF (≤ IIA) and 47 controls (13 healthy skin, 35 BID) (Supplementary Table S1) using the NanoString nCounter Human Myeloid Innate Immunity Panel v2 spiked with 30 customized genes (Supplementary Materials and Methods; Supplementary Table S2). Patients were included using conventional clinical and histopathological criteria. Patient consent for experiments was not required because retrospective studies are exempted according to Danish laws. Based on the 535 most differentially expressed genes ($\sigma/\sigma_{max} > 0.2$), an overall good separation of early-stage MF (early-MF), BID, and healthy skin was observed (Supplementary Figure S1a), and a direct comparison of early-MF and BID (*t*-test: fold change > 3 and $P < 0.01$) identified 45 differentially expressed genes, of which all except one (*SAA1*) were highly expressed in early-MF compared with BID. Based on these genes, a semi-unsupervised two-way hierarchical clustering revealed almost complete separation of early-MF from BID (Supplementary Figure S1b). To build a minimal diagnostic classifier for early-MF, we tested different combinations of the 45 differentially expressed genes to identify the combination that gave the best classifier performance by 10-fold cross-validation. The final classifier consisted of the two genes *TOX* and *TRAF1* (Figure 1a) with a classification accuracy of 90% (Figure 1c). This two-gene classifier was evaluated in an independent validation cohort of 27 patients with early-MF and 17 patients with BID (Figure 1b), with a classification accuracy of 80% (Figure 1d).

Automated digital quantification of protein expression of TOX and TRAF1 revealed a significant upregulation of both TOX and TRAF1 proteins in early-MF compared with controls ($P < 0.0001$ and $P < 0.0001$, respectively) (Figure 2a and b). TOX protein expression was seen in benign lymphocytes in controls and MF, as well as neoplastic lymphocytes in MF located in Pautrier micro-abscesses and dermis (Figure 2c and d). Previous studies report putative diagnostic and prognostic roles for TOX in MF (Huang et al., 2014; Litvinov et al., 2017; Zhang et al., 2012); however, the diagnostic potential has been questioned as TOX expression is not restricted to CD4$^+$ cells (Schrader et al.,

---

SUPPLEMENTARY MATERIALS AND METHODS

Study subjects and skin samples

Patient enrollment was performed in epidemic areas in the municipalities of Corte de Pedra and Jequiriça, located in the state of Bahia (Brazil). Patients with cutaneous leishmaniasis (CL) presented typical ulcerative skin lesions, and diagnoses were made on the basis of parasite detection by culture aspirate histopathology or the presence of a typical CL lesion plus leishmanin skin test positivity. Blood and tissue specimens were obtained before patients received treatment with antimoniate-*N*-methylglucantime. Biopsies were obtained from the borders of skin lesions of patients with CL (n = 10), and skin samples were collected from healthy subjects (n = 7) submitted to elective plastic surgery.

PBMCs and monocyte-derived macrophages

PBMCs were isolated using Ficoll-Hypaque gradients (GE Healthcare, Uppsala, Sweden). PBMC fractions were collected and washed twice with 1 × PBS at 300g for 10 minutes. A representative portion of these cells was labeled with APC-conjugated mAb α-CD14 (clone 61D3) (Sigma Aldrich, St. Louis, MO). Flow cytometry was employed to determine monocyte frequency in each sample and adjusted to 1 × 10^6 CD14$^+$ cells per well to obtain differentiated macrophages at identical proportions. For macrophage differentiation, cells were incubated at 37 °C under 5% carbon dioxide for 2 hours to achieve adhesion. Then, PBMCs were washed to remove any nonadherent cells and maintained in culture with complete RPMI (supplemented with 2 mM L-glutamine, 1 mM sodium pyruvate, 100 U/ml penicillin, 100 μg/ml streptomycin, and 0.1 mM nonessential amino acids) for 7 days to induce macrophage differentiation.

Macrophage-infected CD8$^+$ and CD4$^+$ T-cell cocultures

Leishmania (Viannia) braziliensis (strain Ba788) promastigotes were cultured in Schneider's Insect medium (Sigma Aldrich) (supplemented with 10% fetal bovine serum, 2 mM L-glutamine, 100 U/ml penicillin, and 100 μg/ml streptomycin). Cultured macrophages from patients with CL and healthy subjects were infected with *L. braziliensis* (1:10 macrophage-to-promastigote ratio). After 2 hours of infection, cells were washed to remove any noninternalized promastigotes, followed by coculturing with CD8$^+$ and CD4$^+$ T cells (5:1 cell-to-macrophage ratio) for variable durations as indicated in figure legends. CD8$^+$ and CD4$^+$ T-cell isolation was performed in PBMCs using a magnetic bead system (Dynabeads Untouched Human CD8$^+$ T Cells and Untouched Human CD4$^+$ T Cells Dynabeads) in accordance with manufacturer's instructions.

Reagents and culturing protocol

The reagent 3,4-dichloroisocumarin (Sigma Aldrich) was used as a pharmacological inhibitor of granzyme B. The neutralizing antibody (clone δG9) was used to block perforin. In order to confirm inflammasome activation caused by the influx of potassium, a complete RPMI medium with a high concentration of potassium chloride (50 μM) was used for inhibition purposes, with sodium chloride employed as a negative control.

Real-Time qPCR

Total RNA from skin lesions and cell culture lysates was extracted using an miRNeasy Mini Kit (Qiagen, Hilden, Germany). Reverse transcription was performed to synthesize cDNA using 0.5 μg of total RNA, M-MLV reverse transcriptase, and random primers (Invitrogen, Carlsbad, CA). Relative qPCR reactions were performed (StepOnePlus AB, Applied Biosystems, Foster City, CA) on 96-well microtiter plates using SYBR Green Master Mix (Applied Biosystems). Forward and reverse primer sequences are: for Caspase 1 forward (5′-GCTGAGGTTGACATCACAGGCA-3′) reverse (5′-TGCTGTCAGAGGTCTTGTGCTC-3′); Caspase 5 forward (5′-TGTAAAAC GACGGCCAGT-3′) reverse (5′-CAG GAAACAGCTATGCACC-3′); NLRP 3 forward (5′-GATCTTCGCTGCGAT CAACA-3′) reverse (5′-GGGATTC GAAACACGTGCATTA-3′); AIM2 forward (5′-CAACAAGACTTGAACACA ACGAG-3′) reverse (5′-CTCTCAAT GACTGTGCTGGGTA-3′); and β-actin forward (5′-CACCATTGGCAAT GAGCGGTTC-3′) reverse (5′-AGGT CTTTGCGGATGTCCACGT-3′). All primers were purchased from Applied Biosystems. Samples were amplified in duplicate, and relative expression was calculated as mean comparative computer tomography method for each gene using StepOne Software v2.0.2 (Applied Biosystems). β-actin gene was used as an internal control. All reagents were used in accordance with the manufacturer's recommendations.

IL-1β and active CASP1 quantification

To measure cytokine production in cocultures, supernatants were collected after 12 hours of culturing. IL-1β (Human IL-1β and/or IL-1F2 DuoSet ELISA Development System; R&D Systems, Minneapolis, MI) and active CASP-1 (Human CASP-1/ICE Quantikine ELISA Kit; R&D Systems) concentrations were determined by ELISA sandwich assays in accordance with the manufacturer's instructions. IL-1 β and CASP-1 were measured in the supernatants of patients with CL biopsy cultures after 72 hours of incubation, as previously described by Santos et al. (2018). Briefly, biopsy samples were cultured in complete RPMI media without stimuli at 37 °C, 5% carbon dioxide for 72 hours. Supernatants were collected and stored at −70 °C until the time of analysis by ELISA (R&D Systems) in accordance with the manufacturer's instructions.

Macrophage FAM-FLICA assay

After 12 hours of coculturing, cells were stained with FAM-FLICA FITC reagents in accordance with manufacturer's instructions to determine CASP-1 activation in infected MØ (iMØ) and MØ (FAM-FLICA Caspase-1 Assay Kit, Immunochemistry Technologies, Bloomington, MN). In addition, cells were labeled with phycoerythrin anti-human CD3 mouse antibody (clone SP34-2), phycoerythrin-Cy5−conjugated mAb α-CD8 (clone RPA-T8), and APC-conjugated mAb α-CD14 (clone 61D3) (Sigma Aldrich). A total of 10^5 gated events from each sample were acquired on a FACS Canto II cytometer (BD-Bioscience Pharmingen, San Jose, CA) and analyzed using FlowJo TreeStar software.

Statistical analysis

To analyze relative gene expression in skin lesions and PBMC cultures and cocultures, Mann−Whitney *U* test was used. The Mann−Whitney *U* test was also used to assess differences in IL-1β

and active CASP-1 production by ELISA in all experiments. Comparison of CASP-1 and FLICA positive cells of multiple groups in the presence or absence of different inhibitors were analyzed by Kruskal–Wallis test, followed by Dunn's multiple comparisons post-test. Pearson's coefficient testing was performed to assess correlations between patients with CL healing time and CASP-1 or IL-1β production. All statistical analyses were performed using GraphPad Prism 8.0 software (GraphPad Software, San Diego, CA). *P*-values < 0.05 were considered significant.